SCANNING:
The Journal of Scanning Microscopies

High-Speed Atomic Force Microscopy with Phase-detection

Journal:	*Scanning*
Manuscript ID:	Draft
Wiley - Manuscript type:	Original Article
Date Submitted by the Author:	n/a
Complete List of Authors:	Lee, Donghyeok Lee, Hyunsoo Lee, N. S. Kim, K. B. Seo, Yongho; Sejong University, Nano Science & Technology
Keywords:	AFM/other scanned probe microscopes, Scanned Probe

High-Speed Atomic Force Microscopy with Phase-detection

Donghyeok Lee, Hyunsoo Lee, N. S. Lee, K. B. Kim and Yongho Seo*

Faculty of Nanotechnology and Advanced Material Engineering, Sejong University, Seoul, 143-747, South Korea

Abstract

In order to improve the scanning speed of tapping mode AFM, we have studied the phase-detection mode AFM with a high frequency (1.5 MHz) cantilever. The phase shifts versus tip-sample distance with different types of samples including polymer, semiconductor, and graphite were measured and the interaction forces were analyzed. It was found that the phase shift in repulsive region is nearly linear as a function of distance, which can be used for feedback control in general, except that some blunt tips cause reversed polarity of phase shift due to excessive energy dissipation. High-speed image with scan rate of 100 Hz was obtained which were controlled with phase shift as a feedback signal.

*corresponding author: yseo@sejong.ac.kr

Introduction

Though the atomic force microscopy (AFM) is considered as a very essential technique for nano-characterization and nano-manipulation fields, its slow imaging rate is a critical disadvantage to be utilized in industrial and multidisciplinary research area. In this context, some groups have studied on the high-speed AFM including mechanical feedback contact-mode AFM (C-AFM) [1-3] and small cantilever based non-contact (or tapping mode) AFM (NC-AFM) [4-6].

In case of C-AFM, the response time of the cantilever is determined by the mass of the cantilever and force between the tip and sample [7]. On the other hand, the response time of the cantilever for NC-AFM is complicated depending on whether it is amplitude detection, phase detection, or frequency detection. In case of amplitude detection, the amplitude change has delay time $\tau = Q/\pi f_0$, where Q is the quality factor and f_0 is the resonance frequency of the cantilever [8]. For the frequency detection mode, generally a phase-locked-loop (PLL) circuit is used to measure the frequency shift and the bandwidth of the PLL limits the speed of the AFM. In case of phase-detection mode, however, it is not clear what the bottleneck of the scanning speed is. Theoretically, the response delay time of the phase shift is considered as nearly zero, that is, the instantaneous change occurs in each oscillation cycle [8].

Among many groups who have studied the high-speed NC-AFM, the instrumentation researches on the phase-detection mode were rare. A phase change detection using quartz resonator was reported, where the negative phase change -0.1° corresponding to attractive force was detected [9]. This attractive force detection means that the phase shift is much more sensitive to the interaction forces than the amplitude. The phase shifts are related with viscosity, elasticity, adhesion, hydrophobicity, and surface charges [10,11]. Uchihashi, et al.

reported on fast phase imaging NC-AFM, which detected the phase shift with a bandwidth over 1 MHz [11]. They obtained topography and phase image simultaneously with imaging rate of 100 ms/frame in pure water. Ando, et al. reported a high speed AFM by using phase-modulation mode, where the imaging rate was in the range of 500 ~ 800 ms/frame [12].

Actually the phase shift is not a monotonic function of the interaction force between the tip and sample, but it has different polarities depending on attractive or repulsive forces. The detailed phase-versus-distance behaviors were studied in theoretically and by using computer simulations [13,14]. In order to develop the high-speed phase-detection AFM, the phase shifts as a function of the interaction force with the different types of samples were measured and analyzed at the high frequency regime (≥ 1 MHz) of the cantilever.

Experimental

The cantilever (Arrow UHF, Nanoworld) with 1.5 MHz resonance frequency was used, which is 35 μm long and 42 μm wide. A homemade RT-AFM setup previously reported by our group [7] was used for imaging and phase spectroscopy measurements. The main body of the RT-AFM was composed of head, PZT tube scanner, optical microscope, and coarse approach mechanism (Picomotor, New focus Inc.) The head consisted of laser diode, lens, mirror, and position sensitive photodiode (PSPD). For the PSPD the quad-cells segmented photodiode (OSI optoelectronics, SPOT-4D) was used for high-speed signal detection, as it has 3 ns rising time and 5 pF capacitance. To measure the amplitude and phase simultaneously with wide bandwidth, a lock-in amplifier (SR-844, SRS Inc.) with minimum 10 μs time constant was used.

An analog controller was prepared to control z-directional position of the tube scanner by using the phase shift signal measured by the lock-in amplifier. The controller with 10 μs time constant is composed of 6 op-amps (AD713) operating with proportional-integral control scheme and two polarity switches, as shown in Fig. 1. In other to adapt the polarity change of the phase shift in case, two switches (in dotted boxes) were inserted. The switch 1 is for polarity selection of error signal, and the switch 2 is for the z-scanner direction selection. For example, if the phase decreases as the tip approaches, then both of switches should be down, and vice versa.

Result and discussion

One can simply estimate the phase shift polarity from the harmonic approximation, in which the cantilever motion is approximated as a harmonic oscillator with driven force [8]. From the harmonic approximation, the amplitude always decreases under both attractive (positive force gradient) and repulsive (negative force gradient) interactions, when the driving frequency is set to the resonance frequency ($\omega = \omega_0$). However, the phase shift is increased (decreased) in attractive (repulsive) interaction, as shown in Fig. 2 (a-b). In general, the phase φ is defined from the equation of cantilever motion $z = z_0 \cos(\omega t - \varphi)$ when an external force $F_0 \cos(\omega t)$ is applied, that is, the positive increase of φ means the delay of the cantilever response. The harmonic approximation is valid in limited cases: small oscillation amplitude and constant force gradient [8]. As a preliminary test, the amplitude and phase versus frequencies for a cantilever were measured simultaneously in our setup, as shown in Fig. 2(c). The resonance frequency and quality factor of this cantilever are estimated to be about 1.27 MHz and 70, respectively.

The phase-distance curve measurements were performed on various samples: polycarbonate, Si wafer, highly oriented pyrolytic graphite (HOPG), with high frequency cantilevers. Figures 3 show the amplitude (a) and phase (b) versus distance measurement results. While the amplitude curves show monotonic decreases as it approaches the samples, the phase curves have slight dips (attractive region) and sharp increases (repulsive region), as expected in the harmonic approximation. Note that the phase θ in this data is defined from the cantilever motion $z = z_0 \cos(\omega t - \pi/2 + \theta)$, that is, when θ =0, the cantilever motion is delayed with 90^o and positive value of θ means the earlier response than 90^o.

The phase shift as a function of distance has not been studied as much as the amplitude, theoretically. Particularly, Lee and Jhe studied the phase shift versus distance by calculating numerically an integral equation for dynamic motion of a cantilever [13]. Assuming Lennard-Jones potential with characteristic length *l*, the phase shift as a function of distance (z / l) shows steep increase following gentle decrease for small oscillation region ($A_0 / l = 0.1$), in approaching process. On the other hand, in case of large oscillation amplitude ($A_0 \approx l$), a hysteresis behavior is conspicuous in approaching and retracting cycle. Chen, et al. [15] measured the phase shift on mica (stiff) and polystyrene (soft), in which the resonance frequencies were 85 and 300 kHz, corresponding to the cantilever stiffness of 3 and 40 N/m. Referring to their computer simulation results, for 40 N/m cantilever, the phase slope for a stiff sample was higher, while for 3 N/m cantilever, a soft sample caused a deeper attractive dip and the slope was steeper, that is, complicated results depending on the stiffness of cantilever were reported.

Overall shapes of phase shift curves measured in our experiment are similar to the results of other researcher [13-17]. In our experiment, it was quite difficult to obtain consistent quantitative data for the sample dependence of the phase shift, because the phase shifts were very sensitive to external conditions: tip sharpness, mechanical noise, and laser beam alignment. Particularly, in case of the polycarbonate sample, the phase shift polarity was reversed, (negative slope) occasionally when it was measured by blunt tips. As the polycarbonate is a polymer material, it is expected to have relatively strong internal frictional force compared with the other samples.

In order to acquire more quantitative data, we measured 10 data sets with different cantilevers having the same specifications ($f_0 \approx 1.5$ MHz) where each data set was measured more than 5 times at different points and averaged. From the measured amplitude and phase versus distance curve, the slopes in repulsive region were estimated by linear regression. As each set of data has a different value due to the different tip and alignment conditions, the values were normalized so as that the maximum value is set to 1 among the data measured by the same cantilever for different samples. The resultant data for amplitude and phase are shown in table 1. From 1.5 MHz data in the table, the slope for HOPG was largest and that for polycarbonate was smallest. For comparison purpose, the data taken by 300 kHz cantilever are shown together, which show no noticeable sample dependence within the experimental error ranges. The surface of HOPG was freshly cleaved and expected to be atomically flat. It is well known that the frictional force on graphite surface is almost zero, which has been used as a solid lubricant material [18]. Therefore, the HOPG surface gives rise to negligible energy dissipation.

On the other hand, the polycarbonate which is a kind of polymer material is expected to cause larger frictional force. In the repulsive force region, the larger amount of energy dissipation is expected, and the cantilever motion is delayed in addition to the influence of the repulsive interaction [10,19]. Therefore, phase shift was decreased (that is, delayed) as repulsive force is increased, and the slope of phase versus distance curve was lowered. The negative slope for excessively blunt tip is also, attributed to the extremely high energy dissipation. As a whole, the dips in phase curves corresponding to the attractive interaction showed similar depths irrespective of the kind of samples, because the attractive interaction rarely involves the energy dissipation. In case of 300 kHz cantilever, the velocity of the motion is much slower, and the energy dissipation is not expected to be noticeable.

The feasibility study was performed for fast imaging with phase feedback scheme, in comparison with amplitude feedback. With the amplitude feedback scheme, the polycarbonate surface in a commercial compact disk was scanned with the scan rates (lines/sec): slow, 10, 20, 30, 40, and 50 Hz, as shown in Fig. 4(a). The number of pixels was 100x100, and scanned area was 1.5x1.5 μm^2. The detailed topographic features in slow image are not visible in 40 or 50 Hz image. However, in case of phase feedback images shown in Fig. 4(b), fast scan images with scan rate up to 70 Hz show some detailed features, due to fast response of the phase shift.

For another example, high speed topographic images of HOPG surface were taken, as shown in Fig. 5. The images in (a) were taken in amplitude feedback scheme and (b) in phase feedback scheme. The number of pixels was 100x100, and scanned area was 2x2 μm^2. The cantilever vibration amplitude was about 18 nm and phase set point for feedback control was 10^o from the free oscillation phase. While the amplitude-mode images show the background wiggles in fast scanning images, the phase-mode images show almost flat background up to 100 Hz scan rate. Also, a few-layer-graphene step with 2 nm height was clearly resolved in phase-mode up to 100 Hz scan rate. The scan rate of 100 Hz corresponds to the imaging rate 1 s/frame in the case of 100x100 pixels. This speed is not better than Uchihashi et al.'s result of 100 ms/frame [11], but their images were taken by measuring the phase shifts while the feedback control was done by the amplitude signal. The key point of our work is that the distance control was done by phase shift feedback, which has potential applicability for real-time tapping mode AFM.

Conclusion

Phase shifts as a function of distance were measured with different kinds of samples: polymer (polycarbonate), hard (Si), and frictionless (HOPG) surfaces. The phase curves measured with all samples showed slight dips and sharp increases as the tips approach the samples, which are in agreement with theoretically calculated results. Exceptionally, some data showed reversed polarity (continuous decrease as tip approaches sample), which are attributed to the excessive energy dissipation due to blunt tips. A distance control was attained successfully, by using the linear increase of the phase shift. Fast scanning images with scan rate up to 100 Hz were obtained with feedback control of the phase shift, which showed higher resolutions than those obtained by amplitude mode.

Acknowledgment

This work was supported by the National Research Foundation of Korea (NRF) grants funded by the Korea government Ministry of Education, Science and Technology (MEST) Grant No. R01-2008-000-20185-0 and 331-2008-1-C00102. Also this research was supported by Basic Science Research Program (2009-0070725 and 2010-0005393), Priority Research Centers Program (2010-0020207) through NRF funded by MEST, and Ministry of Knowledge Economy Grant No. 10033728.

Figure Captions

Figure 1. Circuit diagram for PI controller. This controller is composed of 6 op-amps (AD713) operating with proportional-integral control scheme and 2 polarity switches.

Figure 2. Illustrations for the amplitude change (a) and phase shift (b) in attractive and repulsive interactions. These estimations are based on the harmonic approximation. (c) shows the experimental data for amplitude and phase as functions of the external driving frequency.

Figure 3. (a) Amplitude and (b) Phase versus distance curves measured on HOPG, Si, and polycarbonate. The amplitude curves show monotonic decreases, and the phase curves show slight decreases and sharp increases. Each data curve was shifted 10 nm in x-axis, to avoid overlapping the data points.

Figure 4. Topographic images of polycarbonate surface in a compact disk obtained by amplitude feedback control with different scanning rates. The phase control images show much detailed resolution with faster scan rate. The pixel size was 100x100, and the scanned area was 1.5x1.5 μm^2.

Figure 5. Topographic images of HOPG with graphite layer step obtained by (a) amplitude and (b) phase feedback control with different scanning rates: slow, 10 Hz, 30 Hz, 50 Hz, 70 Hz, 90 Hz, and 100 Hz from left-top to right-bottom, respectively. The pixel size was 100x100, and the scanned area was 2x2 μm^2.

	f_0	HOPG	Si wafer	Polycarbonate
Relative amplitude shift	300kHz	0.95±0.1	0.99±0.1	0.99±0.1
	1.5MHz	0.89±0.16	0.86±0.16	0.85±0.14
Relative phase shift	300kHz	0.97±0.1	0.92±0.1	0.98±0.1
	1.5MHz	0.90±0.16	0.83±0.21	0.68±0.27

Table 1. Relative values for maximum slopes of amplitude change and phase change as functions of distance.

REFERENCES

[1] A. D. L. Humphris, M. J. Miles, and J. K. Hobbs, A mechanical microscope: High-speed atomic force microscopy, Appl. Phys. Lett. **86**, (2005) 034106.

[2] L. M. Picco, L. Bozec, A. Ulcinas, D. J. Engledew, M. Antognozzi, M. A. Horton, and M. J. Miles, Breaking the speed limit with atomic force microscopy, Nanotechnology 18, (2007) 044030.

[3] G. E. Fantner, G. Schitter, J. H. Kindt, T. Ivanov, K. Ivanova, R. Patel, N. Holten-Andersen, J. Adams, P. J. Thurner, I. W. Rangelow, and P. K. Hansma, Components for high speed atomic force microscopy, Ultramicroscopy 106, (2006) 881.

[4] T. Ando, N. Kodera, E. Takai, D. Maruyama, K. Saito, and Akitoshi, Toda, A high-speed atomic force microscope for studying biological macromolecules, Proc. Nat. Acad. Sci. 98, (2001) 12468.

[5] T. Ando, N. Kodera, Y. Naito, T. Kinoshita, K. Furuta, and Y. Y. Toyoshima, A High-speed Atomic Force Microscope for Studying Biological Macromolecules in Action, ChemPhysChem. 4, (2003) 1196.

[6] M. B. Viani, T. E. Schäffer, G. T. Paloczi, L. I. Pietrasanta, B. L. Smith, J. B. Thompson, M. Richter, M. Rief, H. E. Gaub, K. W. Plaxco, A. N. Cleland, H. G. Hansma, and P. K. Hansma, Fast imaging and fast force spectroscopy of single biopolymers with a new atomic force microscope designed for small cantilevers, Rev. Sci. Instrum. 70, (1999) 4300.

[7] Y. Seo, C. S. Choi, S. H. Han, and S. J. Han, Real-time atomic force microscopy using

mechanical resonator type scanner, Rev. Sci. Instrum. 79, (2008) 103703.

[8] Y. Seo and W. Jhe, Atomic force microscopy and spectroscopy, Rep. Prog. Phys. 71, (2008) 016101.

[9] R. Nishi, I. Houda, T. Aramata, Y. Sugawara, and S. Morita, Phase change detection of attractive force gradient by using a quartz resonator in noncontact atomic force microscopy, Appl. Surf. Sci. 157, (2000) 332.

[10] J. P. Cleveland, B. Anczykowski, A. E. Schmid, and V. B. Elings, Energy dissipation in tapping-mode atomic force microscopy, Appl. Phys. Lett. **72**, (1998) 2613.

[11] T. Uchihashi, T. Ando, and H. Yamashita, Fast phase imaging in liquids using a rapid scan atomic force microscope, Appl. Phys. Lett. **89**, (2006) 213112.

[12] T. Ando, T. Uchihashi, and T. Fukuma, High-speed atomic force microscopy for nano-visualization of dynamic biomolecular processes, Prog. Surf. Sci. **83** (2008) 337.

[13] M. Lee and W. Jhe, General Theory of Amplitude-Modulation Atomic Force Microscopy, Phys. Rev. Lett. **97**, (2006) 036104.

[14] B. Anczykowski, D. Krüger, K. L. Babcock and H. Fuchs, Basic properties of dynamic force spectroscopy with the scanning force microscopy in experiment and simulation, Ultramicroscopy **66**, (1996) 251.

[15] X. Chen, M. C. Davies, C. J. Roberts, S. J. B. Tendler, P. M. Williams, and N. A. Burnham, Optimizing phase imaging via dynamic force curves, Surf. Sci. 460, (2000) 292.

[16] S. I. Lee, S.W. Howell, A. Raman, and R. Reifenberger, Nonlinear dynamic perspectives on dynamic force microscopy, Ultramicroscopy **97** (2003) 185.

[17] Y. Sugawara, N. Kobayashi, M. Kawakami, Y. J. Li, Y. Naitoh, and M. Kageshima, Appl. Phys. Lett. **90** (2007) 194104.

[18] H. Lee, N. Lee, Y. Seo, J. Eom, and S. Lee, Comparison of frictional forces on graphene

and graphite, Nanotechnology **20**, (2009) 325701.

[19] B. Anczykowski, B. Gotsmann, H. Fuchs, J. P. Cleveland, and V. B. Elings, How to measure energy dissipation in dynamic mode atomic force microscopy, Appl. Surf. Sci. **140**, (1999) 376.

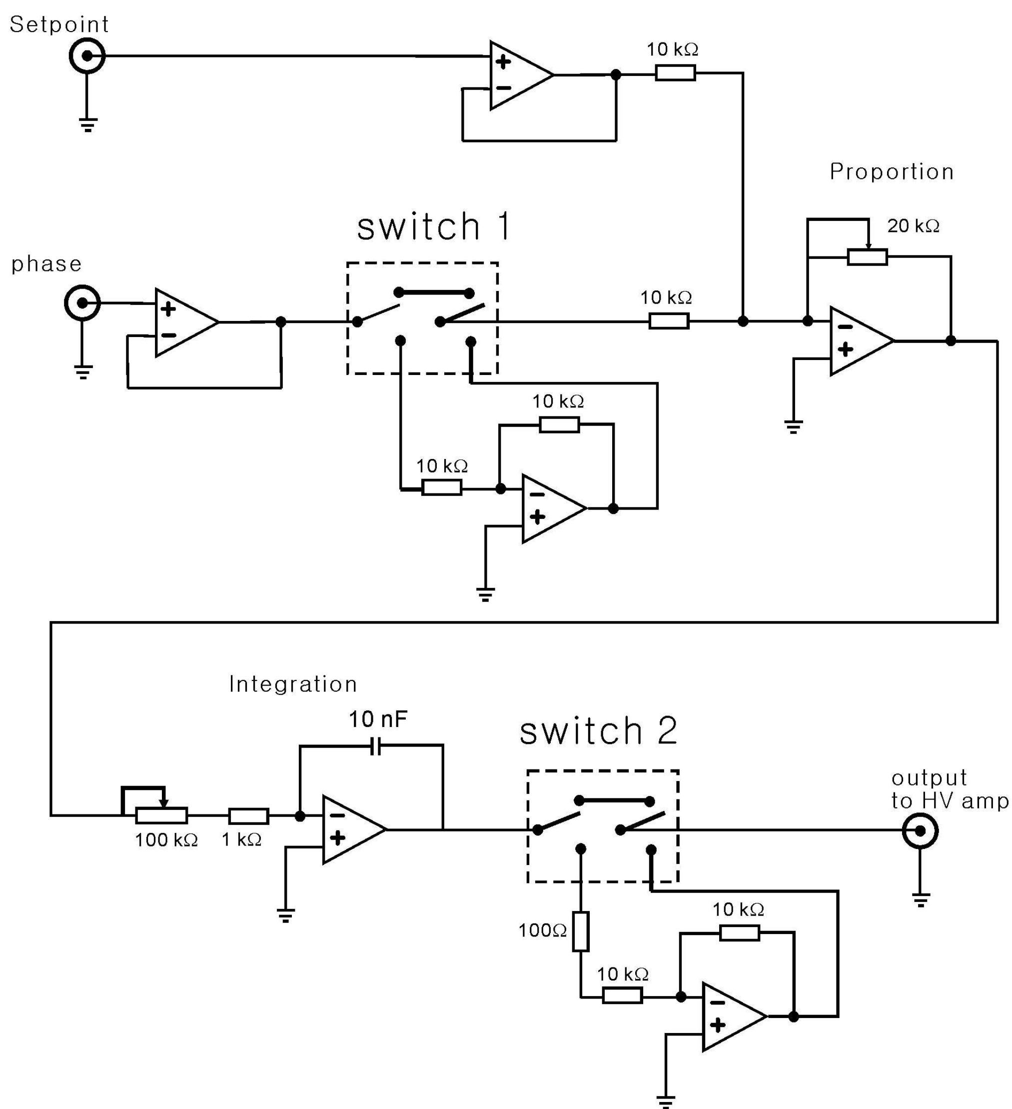

Figure 1. Circuit diagram for PI controller. This controller is composed of 6 op-amps (AD713) operating with proportional-integral control scheme and 2 polarity switches.
158x173mm (300 x 300 DPI)

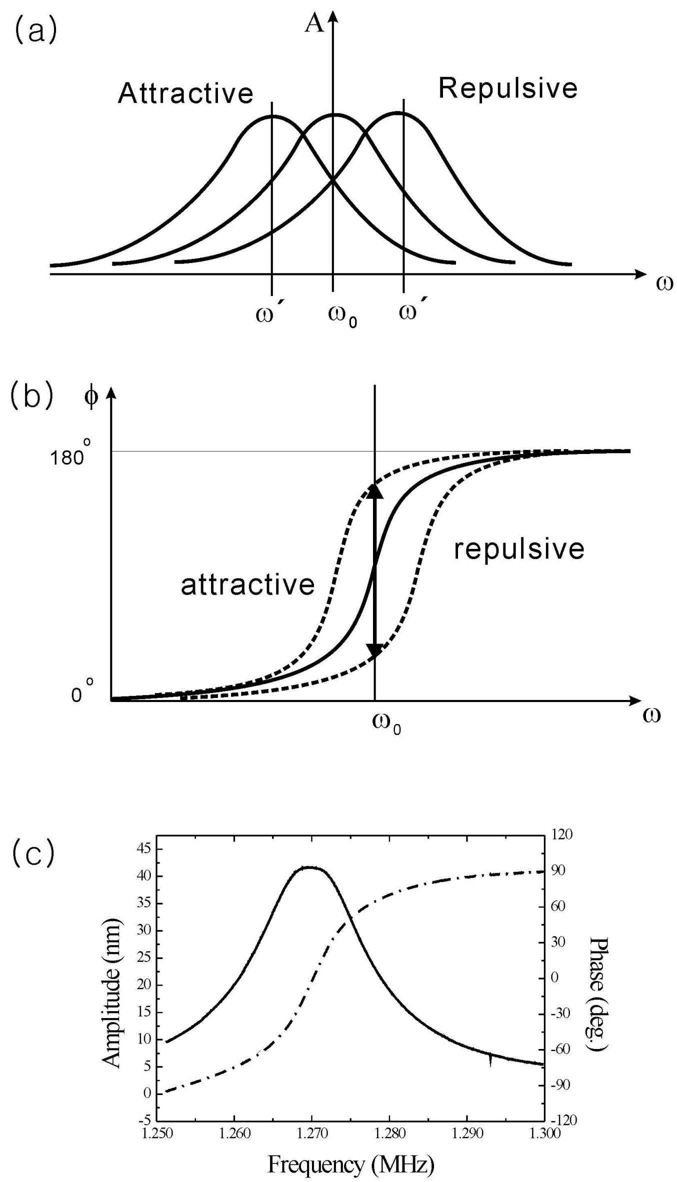

Figure 2. Illustrations for the amplitude change (a) and phase shift (b) in attractive and repulsive interactions. These estimations are based on the harmonic approximation. (c) shows the experimental data for amplitude and phase as functions of the external driving frequency.
138x249mm (300 x 300 DPI)

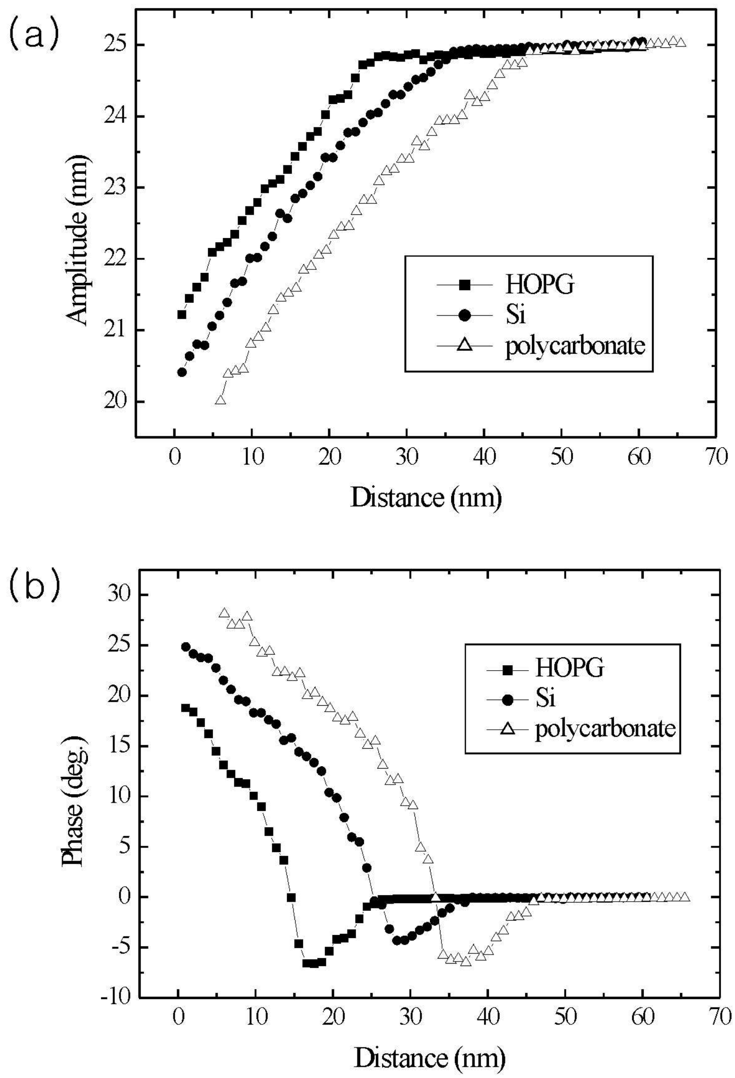

Figure 3. (a) Amplitude and (b) Phase versus distance curves measured on HOPG, Si, and polycarbonate. The amplitude curves show monotonic decreases, and the phase curves show slight decreases and sharp increases. Each data curve was shifted 10 nm in x-axis, to avoid overlapping the data points.
108x162mm (300 x 300 DPI)

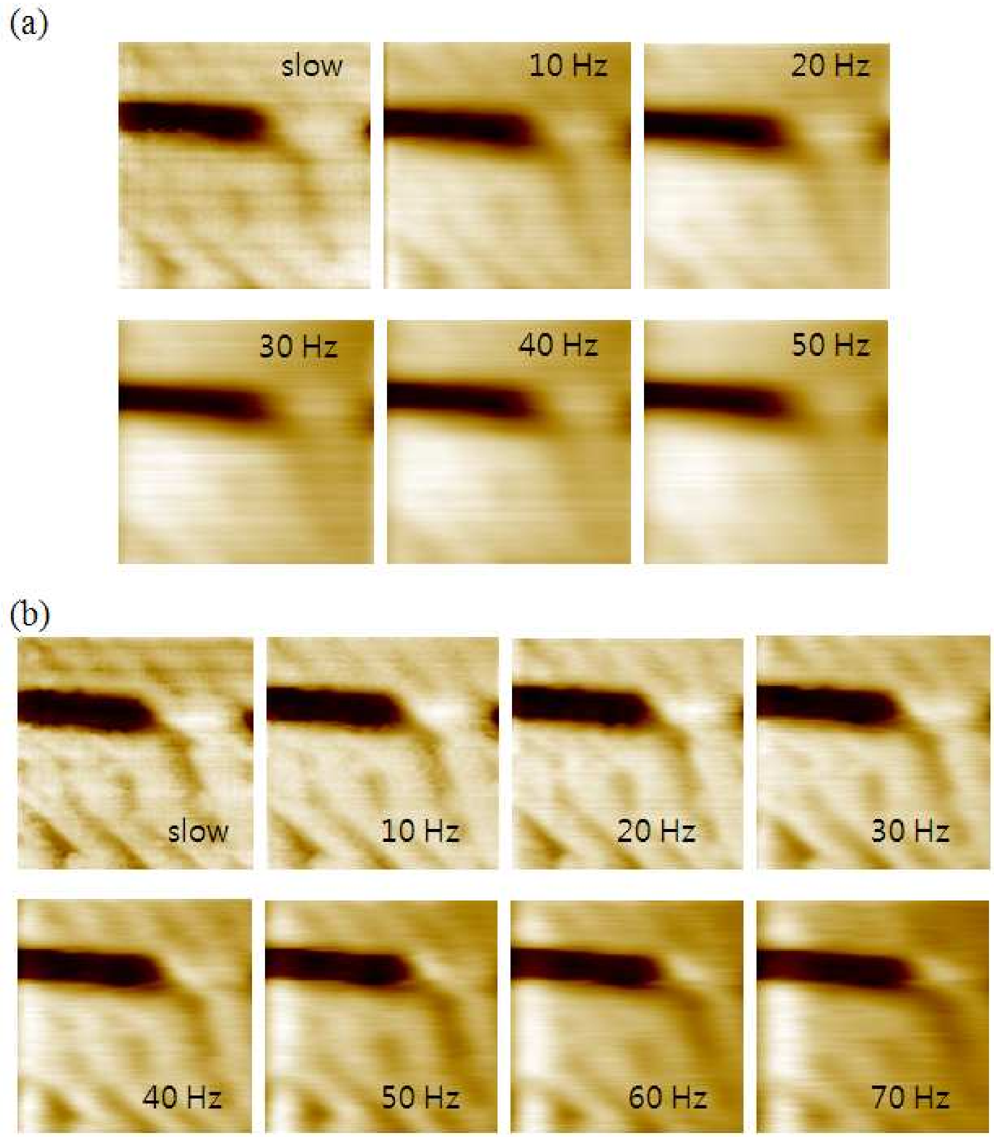

Figure 4. Topographic images of polycarbonate surface in a compact disk obtained by amplitude feedback control with different scanning rates. The phase control images show much detailed resolution with faster scan rate. The pixel size was 100 x 100, and the scanned area was 1.5x1.5 μm^2.
162x190mm (96 x 96 DPI)

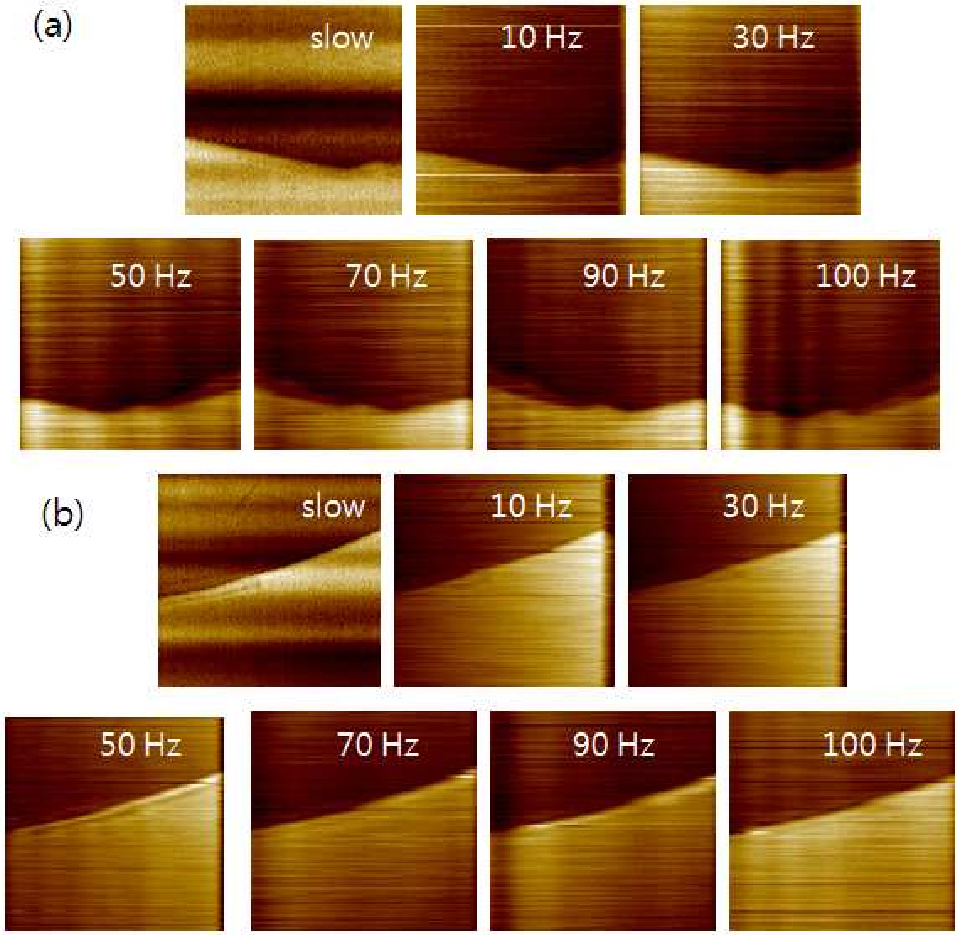

Figure 5. Topographic images of HOPG with graphite layer step obtained by (a) amplitude and (b) phase feedback control with different scanning rates: slow, 10 Hz, 30 Hz, 50 Hz, 70 Hz, 90 Hz, and 100 Hz from left-top to right-bottom, respectively. The pixel size was 100x100, and the scanned area was 2x2 μm^2.
157x153mm (96 x 96 DPI)